

The Repetition Period of MeV Electron Microbursts as measured by SAMPEX/HILT

Hamdan Kandar¹, Lauren W Blum¹, Mykhaylo Shumko², Lunjin Chen³, and Jih-Hong Shue⁴

¹University of Colorado Boulder

²Johns Hopkins University Applied Physics Laboratory

³University of Texas at Dallas

⁴Department of Space Science and Engineering, National Central University

June 14, 2023

Abstract

Here we examine properties of MeV electron microbursts to better understand their generation mechanisms. Using 15 years of data from SAMPEX/HILT, >1MeV microburst repetition periods (time spacing between bursts) are examined and clear dependencies on AE, L shell, and MLT are discovered. Microburst repetition periods are shortest around 0-6 hr MLT and 4-5 Lshell, and grow longer towards the day and afternoon sectors and larger L shells. Shorter repetition periods (<1 sec) are also found to be more common during higher AE, while longer periods (>10 sec) more common during quiet times. The microburst repetition period distributions are compared directly to those of rising tone chorus wave elements and found to be similar in the night, dawn and day MLT sectors, suggesting chorus wave repetition periods are likely directly controlling those of microburst precipitation. However, dusk-side distributions differ, indicating that the dusk-side microbursts properties may be controlled by other processes.

1 **The Repetition Period of MeV Electron Microbursts as measured by**

2 **SAMPEX/HILT**

3 **Hamdan Kandar¹, Lauren Blum^{1,2}, Mykhaylo Shumko³, Lunjin Chen⁴, Jih-Hong Shue⁵**

4 ¹University of Colorado Boulder, Colorado, USA

5 ²Laboratory for Atmospheric and Space Physics, Boulder, Colorado, USA

6 ³The Johns Hopkins University Applied Physics Laboratory, Laurel, MD, USA

7 ⁴University of Texas Dallas, Texas, USA

8 ⁵Department of Space Science and engineering, National Central University, Jhongli, Taiwan

9
10 Corresponding author: Hamdan Kandar (Haka8022@colorado.edu)

11 **Key Points:**

- 12 • The repetition period of MeV electron microbursts is studied for the first time using 15
13 years of SAMPEX/HILT data
- 14 • Microburst repetition periods are most often <1 sec, and drop off as a power law moving
15 to longer periods
- 16 • Repetition periods show strong agreement with chorus wave element periodicities in all
17 MLT sectors except for the dusk sector
- 18

19 Abstract

20 Here we examine properties of MeV electron microbursts to better understand
21 their generation mechanisms. Using 15 years of data from SAMPEX/HILT, >1MeV
22 microburst repetition periods (time spacing between bursts) are examined and clear
23 dependencies on AE, L shell, and MLT are discovered. Microburst repetition periods are
24 shortest around 0-6 hr MLT and 4-5 Lshell, and grow longer towards the day and
25 afternoon sectors and larger L shells. Shorter repetition periods (<1 sec) are also found to
26 be more common during higher AE, while longer periods (>10 sec) more common
27 during quiet times. The microburst repetition period distributions are compared directly
28 to those of rising tone chorus wave elements and found to be similar in the night, dawn
29 and day MLT sectors, suggesting chorus wave repetition periods are likely directly
30 controlling those of microburst precipitation. However, dusk-side distributions differ,
31 indicating that the dusk-side microbursts properties may be controlled by other processes.
32

33 Plain Language Summary

34 Looking at energetic electrons in Earth's magnetosphere from the HILT
35 instrument on board the SAMPEX satellite helps us better understand the feature called
36 microbursts. Microbursts are very rapid bursts of enhanced high-energy electrons
37 entering our atmosphere. In this study, we characterize the properties of the microbursts
38 to understand when, and where they happen, what causes them, and what impact they
39 might have. We do so by looking at factors such as their magnetic local time as well as
40 their time separation. This study also compares these microbursts' results to previous
41 chorus wave studies. Chorus waves have been thought to be related to microbursts and
42 could be a cause for some of their properties. We discuss more about this correlation in
43 the result section of this study.

44 1 Introduction

45 Microbursts are rapid (sub-second) bursts of energetic electrons entering Earth's
46 atmosphere from the magnetosphere. They have been shown to be a significant source of
47 loss for the radiation belts during storm main and recovery phases (e.g. O'Brien et al.
48 2004, Thorne et al. 2005, Breneman et al. 2017, Blum et al. 2015), as well as a potential
49 driver of mesospheric Ozone loss (Seppala et al. 2018, Duderstadt et al. 2021).
50 Microbursts have been observed by numerous spacecraft in low Earth orbits, and can
51 range from keV up to MeV energies (Elliott et al. 2022 and references within).
52 Microbursts occur most frequently between 4 and 6 L shell and from midnight to
53 morning (0 to 12 hr) magnetic local time (MLT) (Lorentzen et al. 2001, Nakamura et al.
54 2000). They typically last on the order of 100 ms, and estimates of the physical size of
55 individual microbursts are on the order of 10 km (e.g. Shumko et al. 2021, Crew et al.
56 2016, Shumko et al. 2018, Shumko et al. 2020).
57

58 Due to their similar distributions in L shell and MLT, as well as their short sub-
59 second durations, rising tone chorus waves have long been considered a primary
60 mechanism for generating microbursts. Chorus waves have been shown to be able to
61 resonate with energetic electrons, rapidly scattering them into the loss cone. Gyro-

62 resonant with keV electrons close to the magnetic equator, and as chorus wave packets
 63 propagate to higher magnetic latitudes they can resonate with higher energy (MeV)
 64 electrons (e.g. Horne and Thorne, 2003, Saito et al. 2012). Simulations as well as a
 65 handful of observations have shown a close correspondence between chorus waves in the
 66 magnetosphere and relativistic electron microbursts at low altitudes (e.g. Chen et al.
 67 2022, Miyoshi et al. 2020, Breneman et al. 2017, Mozer et al. 2017).

68
 69 Microbursts often occur in rapid succession, often referred to as microburst trains
 70 (e.g. O'Brien et al. 2004). It is still an open question what determines the time spacing
 71 (or repetition period) of trains of microbursts, as well as whether isolated microbursts are
 72 generated by the same mechanisms as trains. In this work, we explore the repetition
 73 period of MeV electron microbursts, to gain insight into the possible generation
 74 mechanisms for these repetition periods. Using 15 years of data from the Solar,
 75 Anomalous, Magnetospheric Particles Explorer (SAMPEX) satellite, we calculate the
 76 repetition period of MeV microbursts and examine its dependence on L shell, MLT, and
 77 AE. We then compare these patterns to those found in previous studies of chorus wave
 78 properties.

80 2 Methodology

81 2.1. Detecting microbursts

82
 83 The Solar, Anomalous, Magnetospheric Particles Explorer (SAMPEX) satellite
 84 was designed to measure energetic nuclei and electrons over a broad dynamic range
 85 (Baker et al. 1993). SAMPEX was launched July 3 1992 into an 82 degree inclination
 86 orbit carrying four instruments. We use 20ms cadence measurements of >1 MeV
 87 electrons from the Heavy Ion Large Telescope (HILT) (Klecker et al. 1993) to detect
 88 relativistic electron microbursts from 1997 to 2012.

89
 90 To detect microbursts in the SAMPEX/HILT data, we apply an algorithm
 91 developed by O'Brien et al. (2003) and applied in a number of previous studies:

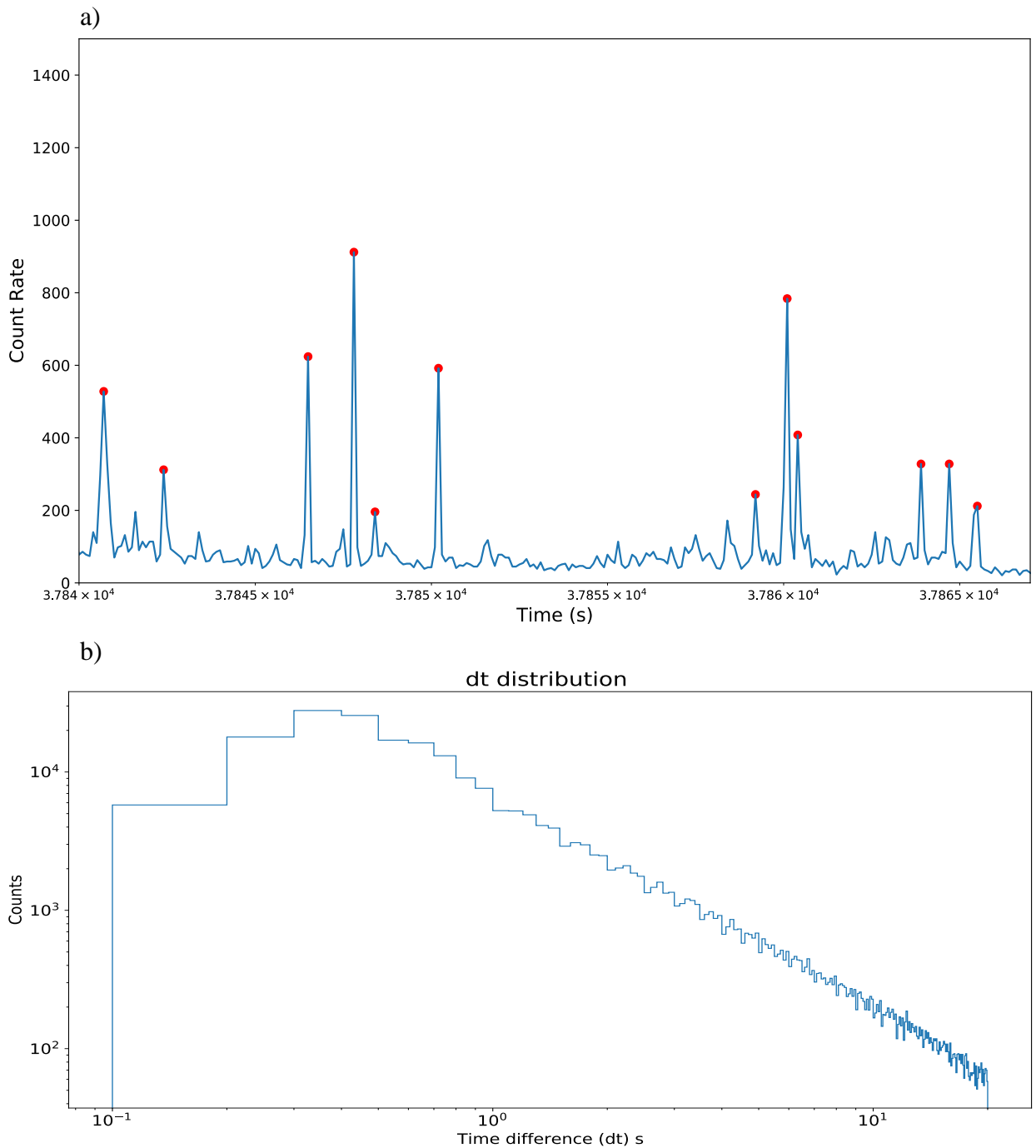
$$(N_{100} - A_{500})/\sqrt{1 + A_{500}} > 10$$

93 where N is the number of counts in 100 ms and A_{500} is a running average over 500 ms.
 94 The threshold of the above ratio set to be 10 so that most microbursts are picked up while
 95 false detections are minimized. For each microburst time, if in the surrounding 250 HILT
 96 samples (nominally 5 seconds), there exists a data gap with duration exceeding 1 second,
 97 we discard that microburst detection, in order to remove false detections near data gaps.
 98 Applying this algorithm to the 15 years analyzed results in a total of 279,061 microburst
 99 detections. This database of microbursts detected by SAMPEX/HILT, while it was in
 100 State 4 (20 ms cadence) and while SAMPEX was not spinning, was compiled by and is
 101 available in Shumko et al. 2021.

102 2.2. Calculating the repetition period

103
 104
 105

106 Once we have the list of microburst detections with assigned date and time, we
107 then calculate the time between each microburst (denoted as dt). Figure 1a shows the
108 application of the O'Brien et al. (2003) microburst detection algorithm as applied to
109 SAMPEX data, as well as how the repetition period (dt) is estimated. Figure 1b shows
110 the overall distribution of dt 's during the 15 year period analyzed. We see from this that
111 most microbursts occur less than one second apart. The number of microbursts drops off
112 as a power law when moving to larger time separations, with slope ~ 0.46 .
113
114



115
116

117

118 **Figure 1.** a) Count rates from SAMPEX HILT (blue) with microbursts detected by the
 119 O'Brien et al. (2003) algorithm (red). The space between the microburst detections
 120 represents the repetition period (dt). b) Distribution of the time difference between
 121 neighboring microbursts in seconds, with both axes on a log scale. Most microbursts
 122 occur less than one second apart.

123 3 Results

124 3.1. L shell and MLT dependence

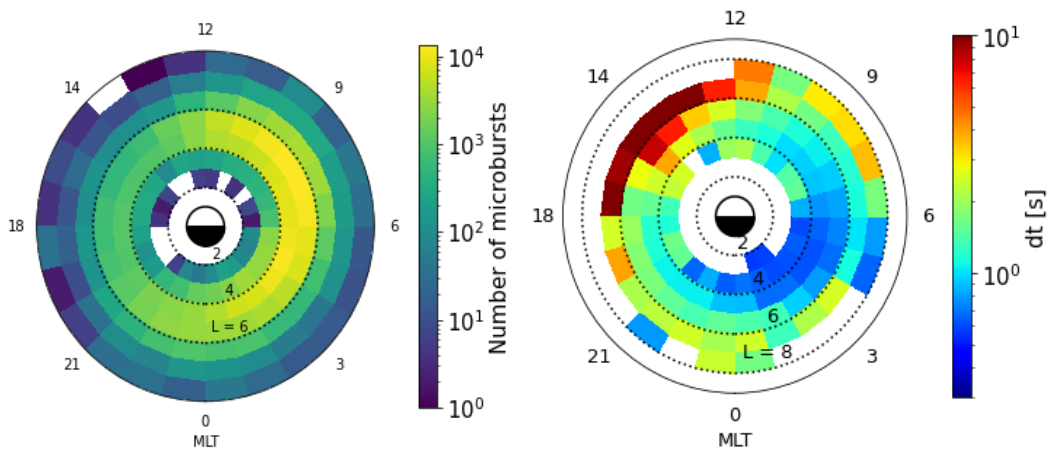
125
 126 With the large database of microbursts and their time separations (dt's) produced
 127 in the steps above, we now explore how the distribution of dt varies with location and
 128 geomagnetic activity.

129
 130 Figure 2a shows the distribution of overall microburst in MLT and L shell. The
 131 number of microburst detections are binned into 1 L by 1 MLT bins. Microbursts are
 132 most frequent on the morning side of the magnetosphere, from ~4-6 L shell, in good
 133 agreement with past studies (O'Brien et al. 2003). This figure also shows that even in the
 134 afternoon sector, more than ~100 detections go into bins from 4-6 L shell, providing
 135 sufficient statistics for examining microburst repetition periods away from their location
 136 of peak occurrence as well.

137
 138 Figure 2b shows the median dt in each MLT-L shell bin. Bins with less than 10
 139 microbursts are white. A clear pattern is evident here, with closely spaced microbursts
 140 located primarily in the dawn sector and at low L shells, while microbursts further
 141 separated in time occur primarily after 12 MLT. The repetition period grows longer as
 142 one moves around in MLT from midnight to noon and to larger L shells. Isolated
 143 microbursts, with unusually longer dt ~ 10 seconds, are often observed at L~6 in the
 144 afternoon sector.

145
 146 a)

b)

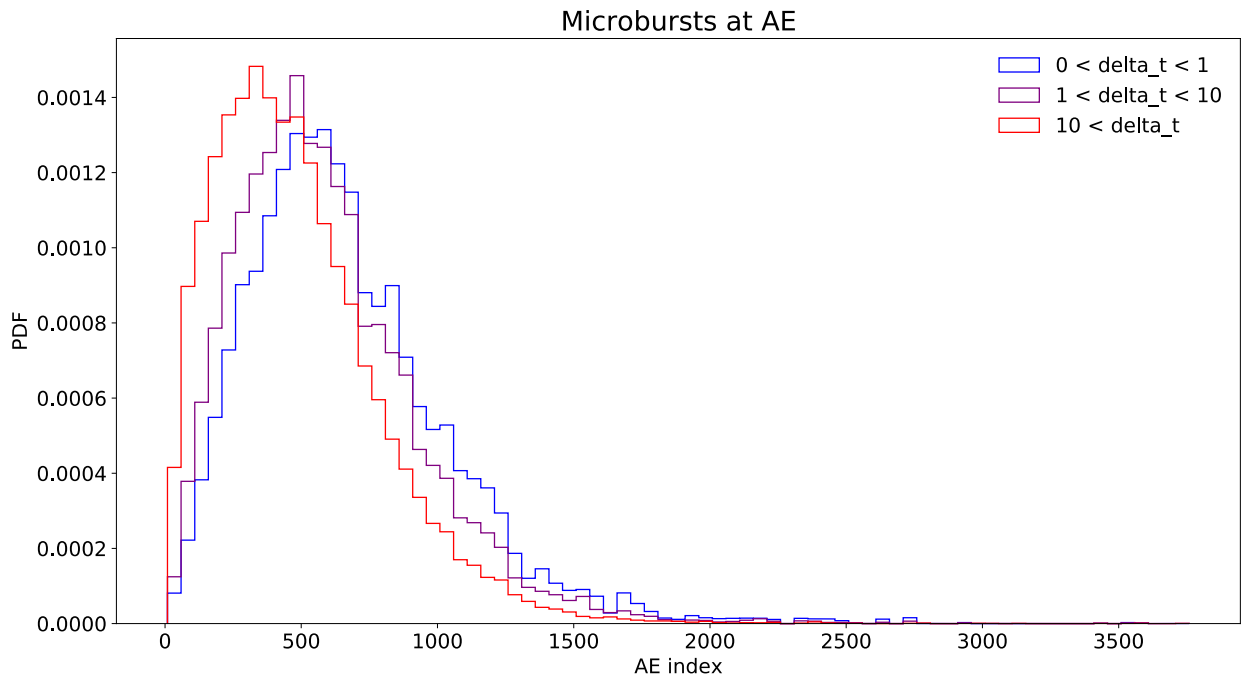


148
 149
 150
 151

152 **Figure 2.** a) Distribution of microbursts in L shell and MLT. b) Distribution of the
 153 median dt in each MLT and L shell bin. Bins with less than 10 microbursts are white.
 154

155 3.2. AE dependence

156
 157 Next, we look at the dependencies of dt on geomagnetic activity, specifically the
 158 Auroral Electrojet (AE) index. Here we sort the microbursts into three categories – those
 159 occurring within 1 second of another microburst, those between 1 and 10 seconds of
 160 another microburst, and those >10 seconds from other microbursts. Figure 3 shows the
 161 microburst repetition period probability density function (PDF) in each of those AE
 162 categories. The width of the AE bins is set to be 50 nT.
 163



164
 165
 166 **Figure 3.** Normalized distribuion of the number of microbursts vs AE index in three
 167 different dt categories. For the dt < 1 second (Blue) the distribution peaks at a value of
 168 559 nT in AE. For 1 < dt < 10s (purple) the peak is at 459 nT in AE. Finally for dt > 10
 169 seconds (red) the peak is 309 nT in AE.
 170

171
 172 The results from Figure 3 reveal that microburst repetition period has an AE
 173 dependency as well. We see that for the dt category of > 10 seconds (red) the curve peaks
 174 at 309 nT in AE, while for the dt category of < 1 second (blue) the curve peaks at 559 nT
 175 in AE. Thus, during active times, when AE is larger, closely spaced microbursts are more
 176 prevalent, while occurrences of more isolated microbursts peak during lower AE values.

177

178 **4 Discussion**

179

180

181

182

183

184

185

186

187

188

189

190

191

192

193

194

195

196

197

198

199

200

201

202

203

204

205

206

207

208

209

210

211

212

213

214

215

216

The results above show clear dependencies of microburst repetition period on MLT, L shell, and AE. To better understand potential causes of these trends in the microburst repetition period, we compare to past studies of this similar repetition period property for chorus waves.

Shue et al. (2015) and Gao et al. (2022) have explored the dependence of rising tone chorus element repetition periods on MLT and both studies found a strong dependence similar to that shown here. Chorus wave repetition periods were shortest in the night and dawn sectors, and longer on the day and duskside. Background magnetic field strength and electron temperature were found to be controlling factors for this chorus repetition period (Shue et al. 2015). Gao et al. (2022) observed an inverse correlation between chorus repetition period and the drift velocity of electrons, suggesting faster drifting electrons produce more rapidly repeating chorus wave elements. Thus the electron refilling rate in a given region, from freshly injected particles on the nightside, directly controls chorus element density (or repetition periods).

Figure 4 shows probability distribution function of microburst dt 's (blue) overlaid with that of chorus waves as derived from Shue et al. (2015) (orange) for the four different MLT sectors. We find very close agreement between these microburst and chorus wave distributions in the night (21-3 hr), dawn (03-09 hr), and day (09-15 hr) MLT sectors, suggesting chorus wave repetition periods are likely directly controlling those of microburst precipitation. This similarity between chorus wave and microburst properties also likely explains the AE dependences found in Figure 3. The refilling rate of freshly injected electrons on the nightside, which provide the free energy for chorus wave generation, is higher during more active geomagnetic conditions, thus resulting in higher repetition period microbursts as compared to quiet times.

Interestingly, we find that the distributions on the duskside (15-21 hr in MLT) do not show the same agreement, indicating that the dusk side microbursts properties may be controlled by processes other than interaction with chorus wave. Meyer-Reed et al. (2023), looking at the pitch angle anisotropy of microbursts rather than repetition period, also found that duskside microburst properties differed from those in other local time sectors. There have also been a few case studies suggesting EMIC waves, rather than chorus waves, may be a possible source of MeV electron microbursts in the dusk sector (e.g. Shumko et al. 2022, Douma et al. 2017). Further investigation into the drivers of dusk-side MeV electron microburst precipitation is needed to better understand the difference demonstrated in Figure 4 between the precipitation properties and those of chorus waves.

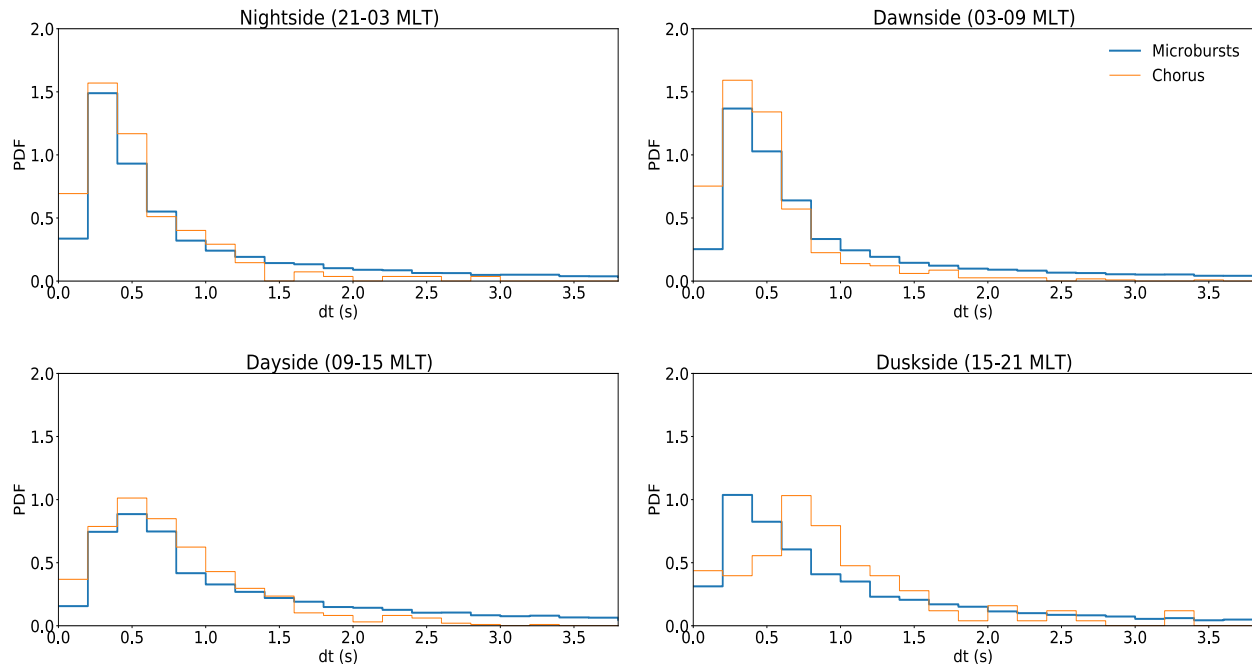


Figure 4. Distributions of the chorus wave (orange) and microbursts (blue) repetition periods in four different MLT categories. Chorus wave distributions are taken from Shue et al. (2015).

217
218
219
220
221

222 5 Summary

223 Here we examine 15 years of SAMPEX data to better understand the detailed properties of
224 MeV electron microbursts, particularly their repetition periods, for the first time. We find:

- 225 1. Microburst repetition periods are most often <1 sec, the distribution follows a decaying
226 power law.
- 227 2. Repetition periods show clear dependencies on MLT, L shell, and AE. The periods peaks
228 near noon and L=4-6, and tend to be shorter for higher AE.
- 229 3. The distribution of microburst dt's shows very strong agreement with that of chorus wave
230 rising tone elements in the night, dawn, and day-side MLT sectors, while dusk-side
231 distributions do not match well.

232 These findings illustrate the insight to be gained from exploring the detailed properties of
233 MeV electron microbursts. The repetition period distributions found here highlight the close
234 connection between chorus wave properties and MeV microburst properties on the night,
235 and day-sides of the magnetosphere, and provide insight into the magnetospheric conditions
236 controlling the trains of microburst precipitation often observed. These findings also reveal the
237 unusual repetition periods of dusk-sector microbursts, suggesting potentially different generation
238 mechanisms or plasma properties mediating the wave-particle interactions in this sector play a
239 role.

240

241

242 **Acknowledgments**

243 This work was supported in part by NASA's H-SR award #80NSSC21K1682, as well as the
244 NASA/Goddard ISFM Space Precipitation Impacts (SPI) team, grant HISFM21. LC
245 acknowledges the support of NASA grant 80NSSC21K1320.

246

247 **Open Research**

248 The sampex data center at Caltech has provided the data which is accessible to the public.
249 Retrieved from <https://izw1.caltech.edu/sampex/DataCenter/index.html> The catalog of
250 SAMPEX/HILT microbursts, and the analysis software used here, is available
251 at: https://github.com/mshumko/sampex_microburst_widths, and is archived on
252 Zenodo <https://doi.org/10.5281/zenodo.5165064>.

253

254 **References**

255 Baker, D. N., Mason, G. M., Figueroa, O., Colon, G., Watzin, J. G., & Aleman, R. M. (1993). An
256 overview of the solar anomalous, and Magnetospheric Particle Explorer (SAMPEX)
257 mission. *IEEE Transactions on Geoscience and Remote Sensing*, 31(3), 531–541.
258 <https://doi.org/10.1109/36.225519>

259 Blum, L., Li, X., & Denton, M. (2015). Rapid MeV electron precipitation as observed by
260 Sampex/hilt during high-speed stream-driven storms. *Journal of Geophysical Research:*
261 *Space Physics*, 120(5), 3783–3794. <https://doi.org/10.1002/2014ja020633>

262 Blum, L. W., and Breneman, A. W. (2020). “Chapter 3—observations of radiation belt losses
263 due to cyclotron wave-particle interactions ”in The dynamic loss of Earth's radiation belts.
264 Tharamani, Chennai: Elsevier. doi:10.1016/B978-0-12-813371-2.00003-2

265 Breneman, A. W., Crew, A., Sample, J., Klumpar, D., Johnson, A., Agapitov, O., Shumko, M.,
266 Turner, D. L., Santolik, O., Wygant, J. R., Cattell, C. A., Thaller, S., Blake, B., Spence, H.,
267 & Kletzing, C. A. (2017). Observations directly linking relativistic electron microbursts to
268 Whistler Mode Chorus: Van allen probes and Firebird II. *Geophysical Research Letters*,
269 44(22). <https://doi.org/10.1002/2017gl075001>

270 Chen, L., Zhang, X. J., Artemyev, A., Angelopoulos, V., Tsai, E., Wilkins, C., & Horne, R. B.
271 (2022). Ducted Chorus waves cause sub-relativistic and relativistic electron microbursts.
272 *Geophysical Research Letters*, 49(5). <https://doi.org/10.1029/2021gl097559>

273

274 Crew, A. B., Spence, H. E., Blake, J. B., Klumpar, D. M., Larsen, B. A., O'Brien, T. P., et al.
275 (2016). First multipoint *in situ* observations of electron microbursts: Initial results from the NSF

- 276 FIREBIRD II mission. *J. Geophys. Res. Space Phys.* 121 (6), 5272–5283.
 277 doi:10.1002/2016ja022485
- 278 Douma, E., Rodger, C. J., Blum, L. W., & Clilverd, M. A. (2017). Occurrence characteristics of
 279 relativistic electron microbursts from Sampex observations. *Journal of Geophysical*
 280 *Research: Space Physics*, 122(8), 8096–8107. <https://doi.org/10.1002/2017ja024067>
- 281 Duderstadt, K. A., Huang, C. -L., Spence, H. E., Smith, S., Blake, J. B., Crew, A. B., Johnson, A.
 282 T., Klumpar, D. M., Marsh, D. R., Sample, J. G., Shumko, M., & Vitt, F. M. (2021).
 283 Estimating the impacts of radiation belt electrons on atmospheric chemistry using Firebird
 284 II and Van Allen probes observations. *Journal of Geophysical Research: Atmospheres*,
 285 126(7). <https://doi.org/10.1029/2020jd033098>
- 286 Elliott, S. S., Breneman, A., Colpitts, C., Bortnik, J., Jaynes, A., Halford, A., Shumko, M., Blum,
 287 L., Chen, L., Greeley, A., & Turner, D. (2022). Understanding the properties, wave drivers,
 288 and impacts of electron microburst precipitation: Current understanding and critical
 289 knowledge gaps. *Frontiers in Astronomy and Space Sciences*, 9.
 290 <https://doi.org/10.3389/fspas.2022.1062422>
- 291 Gao, X., Chen, R., Lu, Q., Chen, L., Chen, H., & Wang, X. (2022). Observational evidence for
 292 the origin of repetitive chorus emissions. *Geophysical Research Letters*, 49(12).
 293 <https://doi.org/10.1029/2022gl099900>
- 294 Horne, R. B., & Thorne, R. M. (2003). Relativistic electron acceleration and precipitation during
 295 resonant interactions with Whistler-Mode Chorus. *Geophysical Research Letters*, 30(10).
 296 <https://doi.org/10.1029/2003gl016973>
- 297 Klecker, B., Hovestadt, D., Scholer, M., Arbinger, H., Ertl, M., Kastele, H., Kuneth, E.,
 298 Laeverenz, P., Seidenschwang, E., Blake, J. B., Katz, N., & Mabry, D. (1993). Hilt: A
 299 heavy ion large area proportional counter telescope for solar and Anomalous Cosmic Rays.
 300 *IEEE Transactions on Geoscience and Remote Sensing*, 31(3), 542–548.
 301 <https://doi.org/10.1109/36.225520>
- 302 Kurita, S., Miyoshi, Y., Blake, J. B., Reeves, G. D., & Kletzing, C. A. (2016). Relativistic
 303 electron microbursts and variations in trapped MeV electron fluxes during the 8–9 October
 304 2012 storm: Sampex and van allen probes observations. *Geophysical Research Letters*,
 305 43(7), 3017–3025. <https://doi.org/10.1002/2016gl068260>
- 306 Lorentzen, K. R., Looper, M. D., & Blake, J. B. (2001). Relativistic electron microbursts during
 307 the gem storms. *Geophysical Research Letters*, 28(13), 2573–2576.
 308 <https://doi.org/10.1029/2001gl012926>
- 309 Meyer-Reed, C., Blum, L., & Shumko, M. (2023). Pitch angle isotropy of relativistic electron
 310 microbursts as observed by SAMPEX/Hilt: Statistical and storm-time properties. *Journal*
 311 *of Geophysical Research: Space Physics*, 128(1). <https://doi.org/10.1029/2022ja030926>

- 312 Miyoshi, Y., Saito, S., Kurita, S., Asamura, K., Hosokawa, K., Sakanoi, T., Mitani, T., Ogawa,
313 Y., Oyama, S., Tsuchiya, F., Jones, S. L., Jaynes, A. N., & Blake, J. B. (2020). Relativistic
314 electron microbursts as high-energy tail of pulsating Aurora electrons. *Geophysical*
315 *Research Letters*, 47(21). <https://doi.org/10.1029/2020gl090360>
- 316 Mozer, F. S., Agapitov, O. V., Blake, J. B., & Vasko, I. Y. (2018). Simultaneous observations of
317 lower band chorus emissions at the equator and microburst precipitating electrons in the
318 ionosphere. *Geophysical Research Letters*, 45(2), 511–516.
319 <https://doi.org/10.1002/2017gl076120>
- 320 Nakamura, R., Isowa, M., Kamide, Y., Baker, D. N., Blake, J. B., and Looper, M. (2000).
321 SAMPEX observations of precipitation bursts in the outer radiation belt. *J. Geophys. Res.* 105
322 (A7), 15875–15885. doi:10.1029/2000JA900018
- 323 O'Brien, T. P. (2003). Energization of relativistic electrons in the presence of Ulf Power and
324 MeV microbursts: Evidence for dual ulf and VLF acceleration. *Journal of Geophysical*
325 *Research*, 108(A8). <https://doi.org/10.1029/2002ja009784>
- 326 O'Brien, T. P., Looper, M. D., and Blake, J. B. (2004). Quantification of relativistic electron
327 microburst losses during the GEM storms. *Geophys. Res. Lett.* 31, L04802.
328 doi:10.1029/2003GL018621
329
- 330 Seppälä, A., Douma, E., Rodger, C., Verronen, P., Clilverd, M. A., and Bortnik, J. (2018).
331 Relativistic electron microburst events: Modeling the atmospheric impact. *Geophys. Res.*
332 *Lett.* 45, 1141–1147. doi:10.1002/2017GL075949
- 333 Shue, J. H., Hsieh, Y. K., Tam, S. W., Wang, K., Fu, H. S., Bortnik, J., Tao, X., Hsieh, W. C., &
334 Pi, G. (2015). Local time distributions of repetition periods for rising tone lower band
335 chorus waves in the magnetosphere. *Geophysical Research Letters*, 42(20), 8294–8301.
336 <https://doi.org/10.1002/2015gl066107>
- 337 Shumko, M., Blum, L. W., & Crew, A. B. (2021). Duration of individual relativistic electron
338 microbursts: A probe into their scattering mechanism. *Geophysical Research Letters*,
339 48(17). <https://doi.org/10.1029/2021gl093879>
- 340 Shumko, M., Sample, J., Johnson, A., Blake, B., Crew, A., Spence, H., Klumpar, D., Agapitov,
341 O., & Handley, M. (2018). Microburst scale size derived from multiple bounces of a
342 microburst simultaneously observed with the Firebird-II CubeSats. *Geophysical Research*
343 *Letters*, 45(17), 8811–8818. <https://doi.org/10.1029/2018gl078925>
- 344 Shumko, M., Gallardo-Lacourt, B., Halford, A. J., Blum, L. W., Liang, J., Miyoshi, Y.,
345 Hosokawa, K., Donovan, E., Mann, I. R., Murphy, K., Spanswick, E. L., Blake, J. B.,
346 Looper, M. D., & Gillies, D. M. (2022). Proton Aurora and relativistic electron microbursts
347 scattered by electromagnetic ion cyclotron waves. *Frontiers in Astronomy and Space*
348 *Sciences*, 9. <https://doi.org/10.3389/fspas.2022.975123>

349 Shumko, M., Johnson, A. T., Sample, J. G., Griffith, B. A., Turner, D. L., O'Brien, T. P.,
350 Agapitov, O., Blake, J. B., & Claudepierre, S. G. (2020). Electron microburst size
351 distribution derived with AeroCube-6. *Journal of Geophysical Research: Space Physics*,
352 125(3). <https://doi.org/10.1029/2019ja027651>

353 Saito, S., Y. Miyoshi, and K. Seki (2012), Relativistic electron microbursts associated with
354 whistler chorus rising tone elements: GEMSIS-RBW simulations, *J. Geophys. Res.*, 117,
355 A10206, doi:10.1029/2012JA018020.

356
357 Thorne, R. M., O'Brien, T. P., Shprits, Y. Y., Summers, D., and Horne, R. B. (2005). Timescale
358 for MeV electron microburst loss during geomagnetic storms. *J. Geophys. Res.* 110, A09202.
359 doi:10.1029/2004JA010882
360

1 **The Repetition Period of MeV Electron Microbursts as measured by**

2 **SAMPEX/HILT**

3 **Hamdan Kandar¹, Lauren Blum^{1,2}, Mykhaylo Shumko³, Lunjin Chen⁴, Jih-Hong Shue⁵**

4 ¹University of Colorado Boulder, Colorado, USA

5 ²Laboratory for Atmospheric and Space Physics, Boulder, Colorado, USA

6 ³The Johns Hopkins University Applied Physics Laboratory, Laurel, MD, USA

7 ⁴University of Texas Dallas, Texas, USA

8 ⁵Department of Space Science and engineering, National Central University, Jhongli, Taiwan

9
10 Corresponding author: Hamdan Kandar (Haka8022@colorado.edu)

11 **Key Points:**

- 12 • The repetition period of MeV electron microbursts is studied for the first time using 15
13 years of SAMPEX/HILT data
- 14 • Microburst repetition periods are most often <1 sec, and drop off as a power law moving
15 to longer periods
- 16 • Repetition periods show strong agreement with chorus wave element periodicities in all
17 MLT sectors except for the dusk sector
- 18

19 Abstract

20 Here we examine properties of MeV electron microbursts to better understand
21 their generation mechanisms. Using 15 years of data from SAMPEX/HILT, >1MeV
22 microburst repetition periods (time spacing between bursts) are examined and clear
23 dependencies on AE, L shell, and MLT are discovered. Microburst repetition periods are
24 shortest around 0-6 hr MLT and 4-5 Lshell, and grow longer towards the day and
25 afternoon sectors and larger L shells. Shorter repetition periods (<1 sec) are also found to
26 be more common during higher AE, while longer periods (>10 sec) more common
27 during quiet times. The microburst repetition period distributions are compared directly
28 to those of rising tone chorus wave elements and found to be similar in the night, dawn
29 and day MLT sectors, suggesting chorus wave repetition periods are likely directly
30 controlling those of microburst precipitation. However, dusk-side distributions differ,
31 indicating that the dusk-side microbursts properties may be controlled by other processes.
32

33 Plain Language Summary

34 Looking at energetic electrons in Earth's magnetosphere from the HILT
35 instrument on board the SAMPEX satellite helps us better understand the feature called
36 microbursts. Microbursts are very rapid bursts of enhanced high-energy electrons
37 entering our atmosphere. In this study, we characterize the properties of the microbursts
38 to understand when, and where they happen, what causes them, and what impact they
39 might have. We do so by looking at factors such as their magnetic local time as well as
40 their time separation. This study also compares these microbursts' results to previous
41 chorus wave studies. Chorus waves have been thought to be related to microbursts and
42 could be a cause for some of their properties. We discuss more about this correlation in
43 the result section of this study.

44 1 Introduction

45 Microbursts are rapid (sub-second) bursts of energetic electrons entering Earth's
46 atmosphere from the magnetosphere. They have been shown to be a significant source of
47 loss for the radiation belts during storm main and recovery phases (e.g. O'Brien et al.
48 2004, Thorne et al. 2005, Breneman et al. 2017, Blum et al. 2015), as well as a potential
49 driver of mesospheric Ozone loss (Seppala et al. 2018, Duderstadt et al. 2021).
50 Microbursts have been observed by numerous spacecraft in low Earth orbits, and can
51 range from keV up to MeV energies (Elliott et al. 2022 and references within).
52 Microbursts occur most frequently between 4 and 6 L shell and from midnight to
53 morning (0 to 12 hr) magnetic local time (MLT) (Lorentzen et al. 2001, Nakamura et al.
54 2000). They typically last on the order of 100 ms, and estimates of the physical size of
55 individual microbursts are on the order of 10 km (e.g. Shumko et al. 2021, Crew et al.
56 2016, Shumko et al. 2018, Shumko et al. 2020).
57

58 Due to their similar distributions in L shell and MLT, as well as their short sub-
59 second durations, rising tone chorus waves have long been considered a primary
60 mechanism for generating microbursts. Chorus waves have been shown to be able to
61 resonate with energetic electrons, rapidly scattering them into the loss cone. Gyro-

62 resonant with keV electrons close to the magnetic equator, and as chorus wave packets
 63 propagate to higher magnetic latitudes they can resonate with higher energy (MeV)
 64 electrons (e.g. Horne and Thorne, 2003, Saito et al. 2012). Simulations as well as a
 65 handful of observations have shown a close correspondence between chorus waves in the
 66 magnetosphere and relativistic electron microbursts at low altitudes (e.g. Chen et al.
 67 2022, Miyoshi et al. 2020, Breneman et al. 2017, Mozer et al. 2017).

68
 69 Microbursts often occur in rapid succession, often referred to as microburst trains
 70 (e.g. O'Brien et al. 2004). It is still an open question what determines the time spacing
 71 (or repetition period) of trains of microbursts, as well as whether isolated microbursts are
 72 generated by the same mechanisms as trains. In this work, we explore the repetition
 73 period of MeV electron microbursts, to gain insight into the possible generation
 74 mechanisms for these repetition periods. Using 15 years of data from the Solar,
 75 Anomalous, Magnetospheric Particles Explorer (SAMPEX) satellite, we calculate the
 76 repetition period of MeV microbursts and examine its dependence on L shell, MLT, and
 77 AE. We then compare these patterns to those found in previous studies of chorus wave
 78 properties.

80 2 Methodology

81 2.1. Detecting microbursts

82
 83 The Solar, Anomalous, Magnetospheric Particles Explorer (SAMPEX) satellite
 84 was designed to measure energetic nuclei and electrons over a broad dynamic range
 85 (Baker et al. 1993). SAMPEX was launched July 3 1992 into an 82 degree inclination
 86 orbit carrying four instruments. We use 20ms cadence measurements of >1 MeV
 87 electrons from the Heavy Ion Large Telescope (HILT) (Klecker et al. 1993) to detect
 88 relativistic electron microbursts from 1997 to 2012.

89
 90 To detect microbursts in the SAMPEX/HILT data, we apply an algorithm
 91 developed by O'Brien et al. (2003) and applied in a number of previous studies:

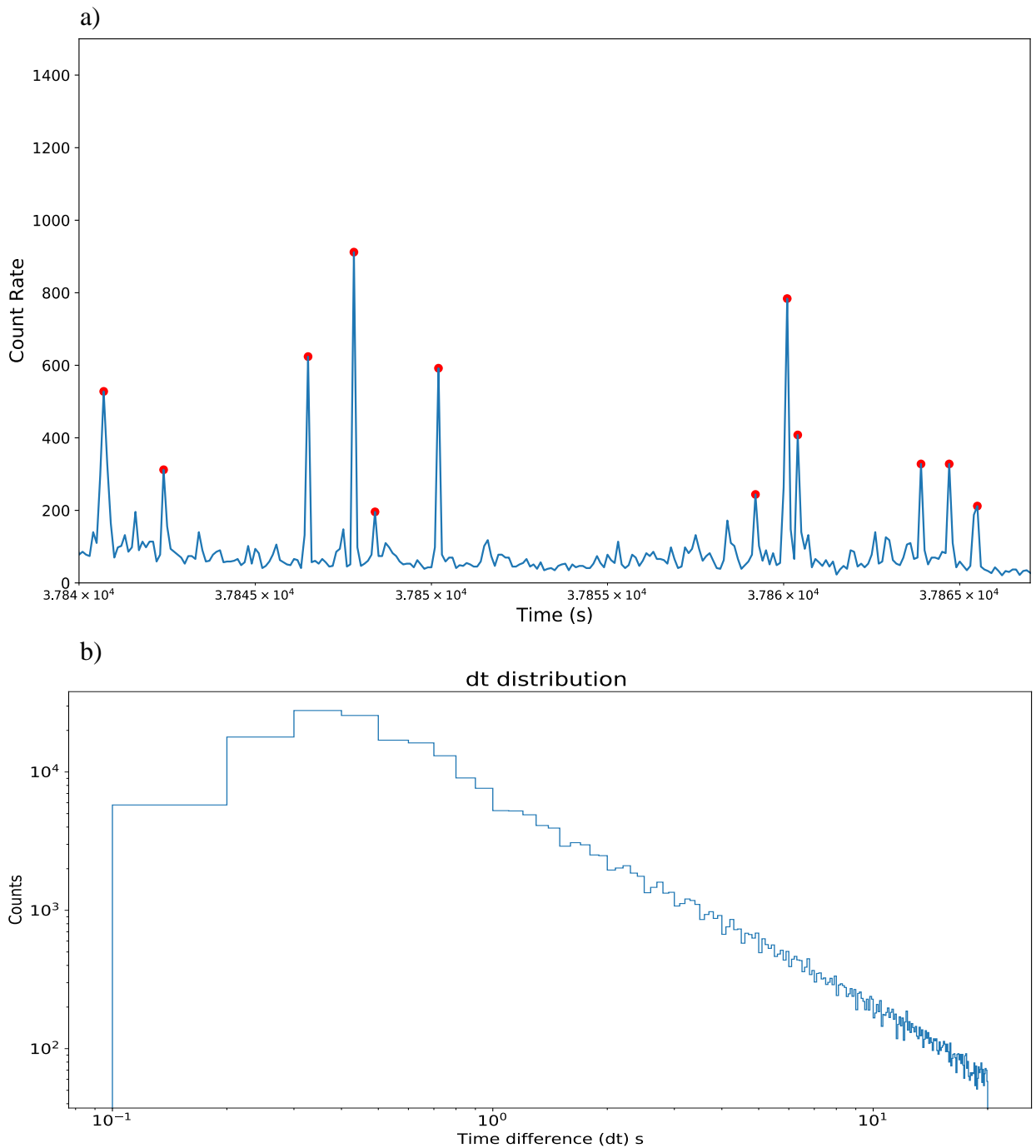
$$(N_{100} - A_{500})/\sqrt{1 + A_{500}} > 10$$

93 where N is the number of counts in 100 ms and A_{500} is a running average over 500 ms.
 94 The threshold of the above ratio set to be 10 so that most microbursts are picked up while
 95 false detections are minimized. For each microburst time, if in the surrounding 250 HILT
 96 samples (nominally 5 seconds), there exists a data gap with duration exceeding 1 second,
 97 we discard that microburst detection, in order to remove false detections near data gaps.
 98 Applying this algorithm to the 15 years analyzed results in a total of 279,061 microburst
 99 detections. This database of microbursts detected by SAMPEX/HILT, while it was in
 100 State 4 (20 ms cadence) and while SAMPEX was not spinning, was compiled by and is
 101 available in Shumko et al. 2021.

102 2.2. Calculating the repetition period

103
 104
 105

106 Once we have the list of microburst detections with assigned date and time, we
107 then calculate the time between each microburst (denoted as dt). Figure 1a shows the
108 application of the O'Brien et al. (2003) microburst detection algorithm as applied to
109 SAMPEX data, as well as how the repetition period (dt) is estimated. Figure 1b shows
110 the overall distribution of dt 's during the 15 year period analyzed. We see from this that
111 most microbursts occur less than one second apart. The number of microbursts drops off
112 as a power law when moving to larger time separations, with slope ~ 0.46 .
113
114



115
116

117

118 **Figure 1.** a) Count rates from SAMPEX HILT (blue) with microbursts detected by the
 119 O'Brien et al. (2003) algorithm (red). The space between the microburst detections
 120 represents the repetition period (dt). b) Distribution of the time difference between
 121 neighboring microbursts in seconds, with both axes on a log scale. Most microbursts
 122 occur less than one second apart.

123 3 Results

124 3.1. L shell and MLT dependence

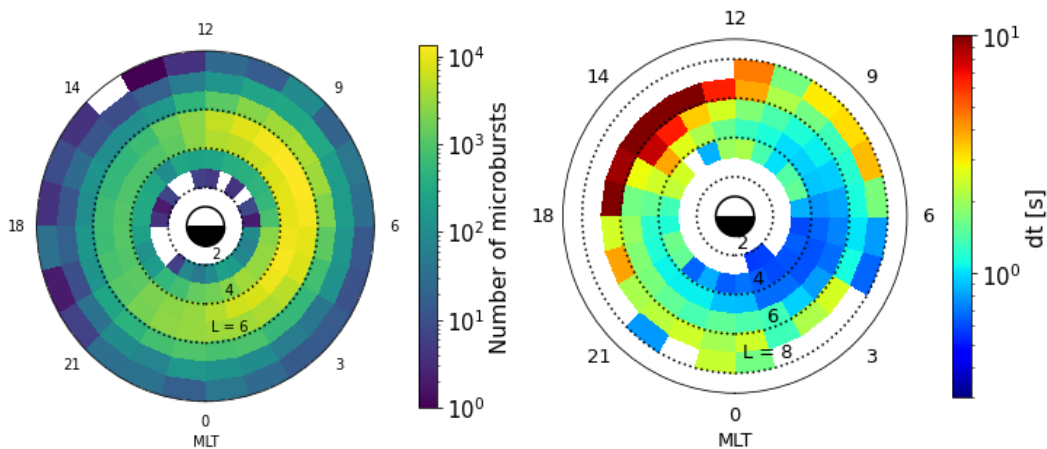
125
 126 With the large database of microbursts and their time separations (dt's) produced
 127 in the steps above, we now explore how the distribution of dt varies with location and
 128 geomagnetic activity.

129
 130 Figure 2a shows the distribution of overall microburst in MLT and L shell. The
 131 number of microburst detections are binned into 1 L by 1 MLT bins. Microbursts are
 132 most frequent on the morning side of the magnetosphere, from ~4-6 L shell, in good
 133 agreement with past studies (O'Brien et al. 2003). This figure also shows that even in the
 134 afternoon sector, more than ~100 detections go into bins from 4-6 L shell, providing
 135 sufficient statistics for examining microburst repetition periods away from their location
 136 of peak occurrence as well.

137
 138 Figure 2b shows the median dt in each MLT-L shell bin. Bins with less than 10
 139 microbursts are white. A clear pattern is evident here, with closely spaced microbursts
 140 located primarily in the dawn sector and at low L shells, while microbursts further
 141 separated in time occur primarily after 12 MLT. The repetition period grows longer as
 142 one moves around in MLT from midnight to noon and to larger L shells. Isolated
 143 microbursts, with unusually longer dt ~ 10 seconds, are often observed at L~6 in the
 144 afternoon sector.

145
 146 a)

b)

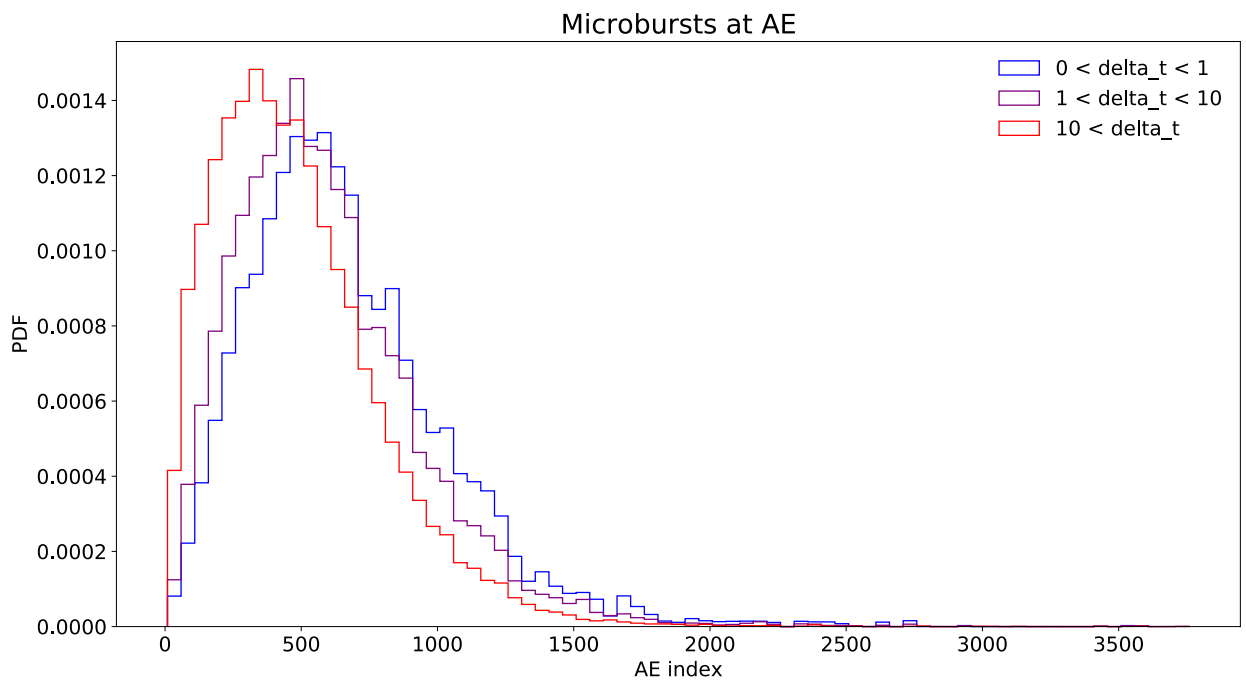


148
 149
 150
 151

152 **Figure 2.** a) Distribution of microbursts in L shell and MLT. b) Distribution of the
 153 median dt in each MLT and L shell bin. Bins with less than 10 microbursts are white.
 154

155 3.2. AE dependence

156
 157 Next, we look at the dependencies of dt on geomagnetic activity, specifically the
 158 Auroral Electrojet (AE) index. Here we sort the microbursts into three categories – those
 159 occurring within 1 second of another microburst, those between 1 and 10 seconds of
 160 another microburst, and those >10 seconds from other microbursts. Figure 3 shows the
 161 microburst repetition period probability density function (PDF) in each of those AE
 162 categories. The width of the AE bins is set to be 50 nT.
 163



164
 165
 166 **Figure 3.** Normalized distribuion of the number of microbursts vs AE index in three
 167 different dt categories. For the dt < 1 second (Blue) the distribution peaks at a value of
 168 559 nT in AE. For 1 < dt < 10s (purple) the peak is at 459 nT in AE. Finally for dt > 10
 169 seconds (red) the peak is 309 nT in AE.
 170

171
 172 The results from Figure 3 reveal that microburst repetition period has an AE
 173 dependency as well. We see that for the dt category of > 10 seconds (red) the curve peaks
 174 at 309 nT in AE, while for the dt category of < 1 second (blue) the curve peaks at 559 nT
 175 in AE. Thus, during active times, when AE is larger, closely spaced microbursts are more
 176 prevalent, while occurrences of more isolated microbursts peak during lower AE values.

177

178 **4 Discussion**

179

180

181

182

183

184

185

186

187

188

189

190

191

192

193

194

195

196

197

198

199

200

201

202

203

204

205

206

207

208

209

210

211

212

213

214

215

216

The results above show clear dependencies of microburst repetition period on MLT, L shell, and AE. To better understand potential causes of these trends in the microburst repetition period, we compare to past studies of this similar repetition period property for chorus waves.

Shue et al. (2015) and Gao et al. (2022) have explored the dependence of rising tone chorus element repetition periods on MLT and both studies found a strong dependence similar to that shown here. Chorus wave repetition periods were shortest in the night and dawn sectors, and longer on the day and duskside. Background magnetic field strength and electron temperature were found to be controlling factors for this chorus repetition period (Shue et al. 2015). Gao et al. (2022) observed an inverse correlation between chorus repetition period and the drift velocity of electrons, suggesting faster drifting electrons produce more rapidly repeating chorus wave elements. Thus the electron refilling rate in a given region, from freshly injected particles on the nightside, directly controls chorus element density (or repetition periods).

Figure 4 shows probability distribution function of microburst dt 's (blue) overlaid with that of chorus waves as derived from Shue et al. (2015) (orange) for the four different MLT sectors. We find very close agreement between these microburst and chorus wave distributions in the night (21-3 hr), dawn (03-09 hr), and day (09-15 hr) MLT sectors, suggesting chorus wave repetition periods are likely directly controlling those of microburst precipitation. This similarity between chorus wave and microburst properties also likely explains the AE dependences found in Figure 3. The refilling rate of freshly injected electrons on the nightside, which provide the free energy for chorus wave generation, is higher during more active geomagnetic conditions, thus resulting in higher repetition period microbursts as compared to quiet times.

Interestingly, we find that the distributions on the duskside (15-21 hr in MLT) do not show the same agreement, indicating that the dusk side microbursts properties may be controlled by processes other than interaction with chorus wave. Meyer-Reed et al. (2023), looking at the pitch angle anisotropy of microbursts rather than repetition period, also found that duskside microburst properties differed from those in other local time sectors. There have also been a few case studies suggesting EMIC waves, rather than chorus waves, may be a possible source of MeV electron microbursts in the dusk sector (e.g. Shumko et al. 2022, Douma et al. 2017). Further investigation into the drivers of dusk-side MeV electron microburst precipitation is needed to better understand the difference demonstrated in Figure 4 between the precipitation properties and those of chorus waves.

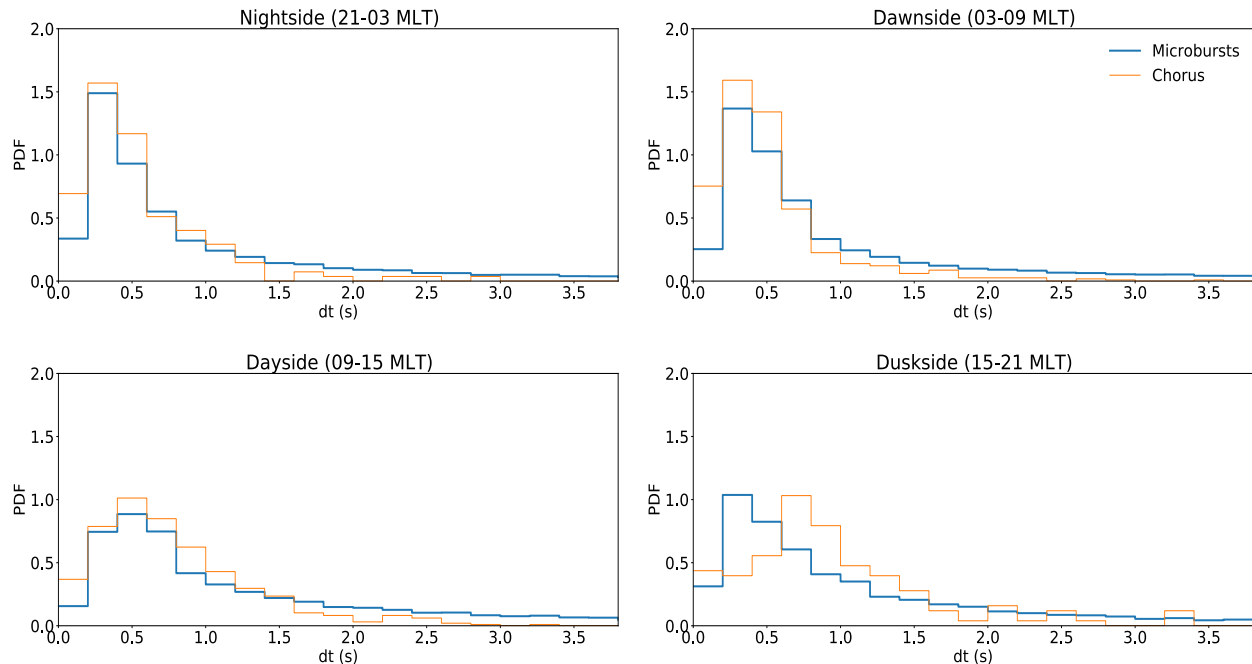


Figure 4. Distributions of the chorus wave (orange) and microbursts (blue) repetition periods in four different MLT categories. Chorus wave distributions are taken from Shue et al. (2015).

217
218
219
220
221

222 5 Summary

223 Here we examine 15 years of SAMPEX data to better understand the detailed properties of
224 MeV electron microbursts, particularly their repetition periods, for the first time. We find:

- 225 1. Microburst repetition periods are most often <1 sec, the distribution follows a decaying
226 power law.
- 227 2. Repetition periods show clear dependencies on MLT, L shell, and AE. The periods peaks
228 near noon and $L=4-6$, and tend to be shorter for higher AE.
- 229 3. The distribution of microburst dt's shows very strong agreement with that of chorus wave
230 rising tone elements in the night, dawn, and day-side MLT sectors, while dusk-side
231 distributions do not match well.

232 These findings illustrate the insight to be gained from exploring the detailed properties of
233 MeV electron microbursts. The repetition period distributions found here highlight the close
234 connection between chorus wave properties and MeV microburst properties on the night,
235 and day-sides of the magnetosphere, and provide insight into the magnetospheric conditions
236 controlling the trains of microburst precipitation often observed. These findings also reveal the
237 unusual repetition periods of dusk-sector microbursts, suggesting potentially different generation
238 mechanisms or plasma properties mediating the wave-particle interactions in this sector play a
239 role.

240

241

242 **Acknowledgments**

243 This work was supported in part by NASA's H-SR award #80NSSC21K1682, as well as the
244 NASA/Goddard ISFM Space Precipitation Impacts (SPI) team, grant HISFM21. LC
245 acknowledges the support of NASA grant 80NSSC21K1320.

246

247 **Open Research**

248 The sampex data center at Caltech has provided the data which is accessible to the public.
249 Retrieved from <https://izw1.caltech.edu/sampex/DataCenter/index.html> The catalog of
250 SAMPEX/HILT microbursts, and the analysis software used here, is available
251 at: https://github.com/mshumko/sampex_microburst_widths, and is archived on
252 Zenodo <https://doi.org/10.5281/zenodo.5165064>.

253

254 **References**

255 Baker, D. N., Mason, G. M., Figueroa, O., Colon, G., Watzin, J. G., & Aleman, R. M. (1993). An
256 overview of the solar anomalous, and Magnetospheric Particle Explorer (SAMPEX)
257 mission. *IEEE Transactions on Geoscience and Remote Sensing*, *31*(3), 531–541.
258 <https://doi.org/10.1109/36.225519>

259 Blum, L., Li, X., & Denton, M. (2015). Rapid MeV electron precipitation as observed by
260 Sampex/hilt during high-speed stream-driven storms. *Journal of Geophysical Research:*
261 *Space Physics*, *120*(5), 3783–3794. <https://doi.org/10.1002/2014ja020633>

262 Blum, L. W., and Breneman, A. W. (2020). "Chapter 3—observations of radiation belt losses
263 due to cyclotron wave-particle interactions "in The dynamic loss of Earth's radiation belts.
264 Tharamani, Chennai: Elsevier. doi:10.1016/B978-0-12-813371-2.00003-2

265 Breneman, A. W., Crew, A., Sample, J., Klumpar, D., Johnson, A., Agapitov, O., Shumko, M.,
266 Turner, D. L., Santolik, O., Wygant, J. R., Cattell, C. A., Thaller, S., Blake, B., Spence, H.,
267 & Kletzing, C. A. (2017). Observations directly linking relativistic electron microbursts to
268 Whistler Mode Chorus: Van allen probes and Firebird II. *Geophysical Research Letters*,
269 *44*(22). <https://doi.org/10.1002/2017gl075001>

270 Chen, L., Zhang, X. J., Artemyev, A., Angelopoulos, V., Tsai, E., Wilkins, C., & Horne, R. B.
271 (2022). Ducted Chorus waves cause sub-relativistic and relativistic electron microbursts.
272 *Geophysical Research Letters*, *49*(5). <https://doi.org/10.1029/2021gl097559>

273

274 Crew, A. B., Spence, H. E., Blake, J. B., Klumpar, D. M., Larsen, B. A., O'Brien, T. P., et al.
275 (2016). First multipoint *in situ* observations of electron microbursts: Initial results from the NSF

- 276 FIREBIRD II mission. *J. Geophys. Res. Space Phys.* 121 (6), 5272–5283.
 277 doi:10.1002/2016ja022485
- 278 Douma, E., Rodger, C. J., Blum, L. W., & Clilverd, M. A. (2017). Occurrence characteristics of
 279 relativistic electron microbursts from Sampex observations. *Journal of Geophysical*
 280 *Research: Space Physics*, 122(8), 8096–8107. <https://doi.org/10.1002/2017ja024067>
- 281 Duderstadt, K. A., Huang, C. -L., Spence, H. E., Smith, S., Blake, J. B., Crew, A. B., Johnson, A.
 282 T., Klumpar, D. M., Marsh, D. R., Sample, J. G., Shumko, M., & Vitt, F. M. (2021).
 283 Estimating the impacts of radiation belt electrons on atmospheric chemistry using Firebird
 284 II and Van Allen probes observations. *Journal of Geophysical Research: Atmospheres*,
 285 126(7). <https://doi.org/10.1029/2020jd033098>
- 286 Elliott, S. S., Breneman, A., Colpitts, C., Bortnik, J., Jaynes, A., Halford, A., Shumko, M., Blum,
 287 L., Chen, L., Greeley, A., & Turner, D. (2022). Understanding the properties, wave drivers,
 288 and impacts of electron microburst precipitation: Current understanding and critical
 289 knowledge gaps. *Frontiers in Astronomy and Space Sciences*, 9.
 290 <https://doi.org/10.3389/fspas.2022.1062422>
- 291 Gao, X., Chen, R., Lu, Q., Chen, L., Chen, H., & Wang, X. (2022). Observational evidence for
 292 the origin of repetitive chorus emissions. *Geophysical Research Letters*, 49(12).
 293 <https://doi.org/10.1029/2022gl099900>
- 294 Horne, R. B., & Thorne, R. M. (2003). Relativistic electron acceleration and precipitation during
 295 resonant interactions with Whistler-Mode Chorus. *Geophysical Research Letters*, 30(10).
 296 <https://doi.org/10.1029/2003gl016973>
- 297 Klecker, B., Hovestadt, D., Scholer, M., Arbinger, H., Ertl, M., Kastele, H., Kuneth, E.,
 298 Laeverenz, P., Seidenschwang, E., Blake, J. B., Katz, N., & Mabry, D. (1993). Hilt: A
 299 heavy ion large area proportional counter telescope for solar and Anomalous Cosmic Rays.
 300 *IEEE Transactions on Geoscience and Remote Sensing*, 31(3), 542–548.
 301 <https://doi.org/10.1109/36.225520>
- 302 Kurita, S., Miyoshi, Y., Blake, J. B., Reeves, G. D., & Kletzing, C. A. (2016). Relativistic
 303 electron microbursts and variations in trapped MeV electron fluxes during the 8–9 October
 304 2012 storm: Sampex and van allen probes observations. *Geophysical Research Letters*,
 305 43(7), 3017–3025. <https://doi.org/10.1002/2016gl068260>
- 306 Lorentzen, K. R., Looper, M. D., & Blake, J. B. (2001). Relativistic electron microbursts during
 307 the gem storms. *Geophysical Research Letters*, 28(13), 2573–2576.
 308 <https://doi.org/10.1029/2001gl012926>
- 309 Meyer-Reed, C., Blum, L., & Shumko, M. (2023). Pitch angle isotropy of relativistic electron
 310 microbursts as observed by SAMPEX/Hilt: Statistical and storm-time properties. *Journal*
 311 *of Geophysical Research: Space Physics*, 128(1). <https://doi.org/10.1029/2022ja030926>

- 312 Miyoshi, Y., Saito, S., Kurita, S., Asamura, K., Hosokawa, K., Sakanoi, T., Mitani, T., Ogawa,
313 Y., Oyama, S., Tsuchiya, F., Jones, S. L., Jaynes, A. N., & Blake, J. B. (2020). Relativistic
314 electron microbursts as high-energy tail of pulsating Aurora electrons. *Geophysical*
315 *Research Letters*, 47(21). <https://doi.org/10.1029/2020gl090360>
- 316 Mozer, F. S., Agapitov, O. V., Blake, J. B., & Vasko, I. Y. (2018). Simultaneous observations of
317 lower band chorus emissions at the equator and microburst precipitating electrons in the
318 ionosphere. *Geophysical Research Letters*, 45(2), 511–516.
319 <https://doi.org/10.1002/2017gl076120>
- 320 Nakamura, R., Isowa, M., Kamide, Y., Baker, D. N., Blake, J. B., and Looper, M. (2000).
321 SAMPEX observations of precipitation bursts in the outer radiation belt. *J. Geophys. Res.* 105
322 (A7), 15875–15885. doi:10.1029/2000JA900018
- 323 O'Brien, T. P. (2003). Energization of relativistic electrons in the presence of Ulf Power and
324 MeV microbursts: Evidence for dual ulf and VLF acceleration. *Journal of Geophysical*
325 *Research*, 108(A8). <https://doi.org/10.1029/2002ja009784>
- 326 O'Brien, T. P., Looper, M. D., and Blake, J. B. (2004). Quantification of relativistic electron
327 microburst losses during the GEM storms. *Geophys. Res. Lett.* 31, L04802.
328 doi:10.1029/2003GL018621
329
- 330 Seppälä, A., Douma, E., Rodger, C., Verronen, P., Clilverd, M. A., and Bortnik, J. (2018).
331 Relativistic electron microburst events: Modeling the atmospheric impact. *Geophys. Res.*
332 *Lett.* 45, 1141–1147. doi:10.1002/2017GL075949
- 333 Shue, J. H., Hsieh, Y. K., Tam, S. W., Wang, K., Fu, H. S., Bortnik, J., Tao, X., Hsieh, W. C., &
334 Pi, G. (2015). Local time distributions of repetition periods for rising tone lower band
335 chorus waves in the magnetosphere. *Geophysical Research Letters*, 42(20), 8294–8301.
336 <https://doi.org/10.1002/2015gl066107>
- 337 Shumko, M., Blum, L. W., & Crew, A. B. (2021). Duration of individual relativistic electron
338 microbursts: A probe into their scattering mechanism. *Geophysical Research Letters*,
339 48(17). <https://doi.org/10.1029/2021gl093879>
- 340 Shumko, M., Sample, J., Johnson, A., Blake, B., Crew, A., Spence, H., Klumpar, D., Agapitov,
341 O., & Handley, M. (2018). Microburst scale size derived from multiple bounces of a
342 microburst simultaneously observed with the Firebird-II CubeSats. *Geophysical Research*
343 *Letters*, 45(17), 8811–8818. <https://doi.org/10.1029/2018gl078925>
- 344 Shumko, M., Gallardo-Lacourt, B., Halford, A. J., Blum, L. W., Liang, J., Miyoshi, Y.,
345 Hosokawa, K., Donovan, E., Mann, I. R., Murphy, K., Spanswick, E. L., Blake, J. B.,
346 Looper, M. D., & Gillies, D. M. (2022). Proton Aurora and relativistic electron microbursts
347 scattered by electromagnetic ion cyclotron waves. *Frontiers in Astronomy and Space*
348 *Sciences*, 9. <https://doi.org/10.3389/fspas.2022.975123>

349 Shumko, M., Johnson, A. T., Sample, J. G., Griffith, B. A., Turner, D. L., O'Brien, T. P.,
350 Agapitov, O., Blake, J. B., & Claudepierre, S. G. (2020). Electron microburst size
351 distribution derived with AeroCube-6. *Journal of Geophysical Research: Space Physics*,
352 125(3). <https://doi.org/10.1029/2019ja027651>

353 Saito, S., Y. Miyoshi, and K. Seki (2012), Relativistic electron microbursts associated with
354 whistler chorus rising tone elements: GEMSIS-RBW simulations, *J. Geophys. Res.*, 117,
355 A10206, doi:10.1029/2012JA018020.

356
357 Thorne, R. M., O'Brien, T. P., Shprits, Y. Y., Summers, D., and Horne, R. B. (2005). Timescale
358 for MeV electron microburst loss during geomagnetic storms. *J. Geophys. Res.* 110, A09202.
359 doi:10.1029/2004JA010882
360